Quantifying Dextral Shear on the Bristol-Granite Mountains Fault Zone: Successful Geologic Prediction from Kinematic Compatibility of the Eastern California Shear Zone

Richard Oliver Lease,[1] *Nadine McQuarrie, Michael Oskin,*[2] *and Andrew Leier*[3]

Department of Geosciences, Guyot Hall, Princeton University, Princeton, New Jersey 08544, U.S.A. (e-mail: rlease@crustal.ucsb.edu)

ABSTRACT

For regional kinematic compatibility to be a valid boundary condition for continental tectonic reconstructions, there must be tests that validate or invalidate kinematic model predictions. In several reconstructions of western North America, the displacement history of the Mojave block continues to be unresolved. The magnitude of displacement along the Bristol-Granite mountains fault zone (BGMFZ), which is the eastern margin of the Eastern California Shear Zone (ECSZ) in the Mojave block, is a key example of a long-standing kinematic prediction that has defied a positive field test until now. The ECSZ is a network of late Neogene and Quaternary right-lateral strike-slip faults that extend from the Gulf of California north through the Mojave Desert, linking Pacific–North America plate motion with Basin and Range extension. This network of faults accounts for ~15% of post-16-Ma plate transform motion. Geologic estimates of net dextral offset along the Mojave portion of the ECSZ (53 ± 6 km) are approximately half that measured to the north in the Owens Valley–Death Valley region (~100 ± 10 km). Previous geological estimates of BGMFZ slip range from 0 to 15 km. Models of right-lateral displacement that are based on kinematic compatibility suggest 21–27 km of BGMFZ displacement. We map and describe a tuff- and gravel-filled paleovalley offset by the BGMFZ. The orientation of the Lost Marble paleovalley is constrained by the position of gravel outcrops, provenance, and tuff anisotropy of magnetic susceptibility. Reconstruction of the paleovalley indicates at least 24 km of post-18.5-Ma dextral offset, confirming a significant, previously undocumented component of dextral slip in the Mojave portion of the ECSZ.

Online enhancement: appendix.

Introduction

Since the advent of plate tectonics, a major goal of geologists has been to link the relatively precise horizontal kinematics of oceanic plates, using seafloor topographic and magnetic anomalies, to the much more imprecise and diffuse deformation that characterizes the continental portion of plate boundaries (Atwater 1970; Molnar and Tapponnier 1975; Tapponnier et al. 1982; Pardo-Casas and Molnar 1987; Şengör 1990; Atwater and Stock 1998; McQuarrie et al. 2003). However these continental tectonic reconstructions at scales of 100–1000 km are often fraught with large uncertainties because of limited regional strain markers, such as regional structures, widespread volcanic units, changes in stratigraphic facies, and paleomagnetically determined vertical axis rotations (Şengör and Natal'in 1996; Wernicke and Snow 2000; McQuarrie 2002; McQuarrie et al. 2003; Oskin and Stock 2003; McQuarrie and Wernicke 2005). Regional kinematic compatibility is often invoked as the prerequisite boundary condition for continental tectonic reconstructions. However, for kinematic compatibility arguments to be trusted, there must be tests for their predictions, and individual faults within a tectonic model must be examined to determine whether the tectonic model and field data are coherent.

Over the last several years, high-quality, regional kinematic constraints that resulted from decades of

Manuscript received March 28, 2008; accepted September 17, 2008.

[1] Present address: Department of Earth Science, University of California, Santa Barbara, California 93106, U.S.A.; e-mail: rlease@crustal.ucsb.edu.

[2] Department of Geology, University of California, Davis, California 95616, U.S.A.

[3] Department of Geosciences, Guyot Hall, Princeton University, Princeton, New Jersey 08544, U.S.A.; present address: Department of Geoscience, University of Calgary, 2500 University Drive NW, Calgary, Alberta T2N 1N4, Canada.

[The Journal of Geology, 2009, volume 117, p. 37–53] 0022-1376/2009/11701-0004$15.00 DOI: 10.1086/593320

field work (and attending debate) have become available for much of southwestern North America, allowing for a detailed kinematic model of the region (Dickinson and Wernicke 1997; Atwater and Stock 1998; Snow and Wernicke 2000; McQuarrie and Wernicke 2005). However, an outstanding problem with all models of western North America deformation continues to be the displacement history of the Mojave Desert region of southern California. In this article, we focus on the eastern edge of the Mojave block (fig. 1), where kinematic models predict 20–30 km of right-lateral shear (Dokka and Travis 1990*a*; McQuarrie and Wernicke 2005), but known geologic markers suggest much less, 0–15 km (Brady 1992, 1993; Howard and Miller 1992; Miller 1993). The Bristol-Granite mountains fault zone (BGMFZ) along the eastern edge of the Eastern California Shear Zone (ECSZ) in the Mojave province provides a key area to test kinematic models. The purpose of this article is to assess whether field data support the long-standing kinematic prediction for the BGMFZ.

Fault Kinematics of the ECSZ. The ECSZ is a vital link between Basin and Range extension and Pacific–North American plate transform motion (Atwater 1970; Dokka and Travis 1990*b*; Wernicke and Snow 1998), accommodating 15% of post-16-Ma transform motion (McQuarrie and Wernicke 2005). The long-term ECSZ dextral slip rate of 8.3 ± 1 mm/yr (McQuarrie and Wernicke 2005) is similar to geodetic rates of 10–14 mm/yr (Savage et al. 1990; Sauber et al. 1994; McClusky et al. 2001). However, the timing, magnitude, and rate of faulting within the ECSZ over its proposed 12-Ma history are poorly understood.

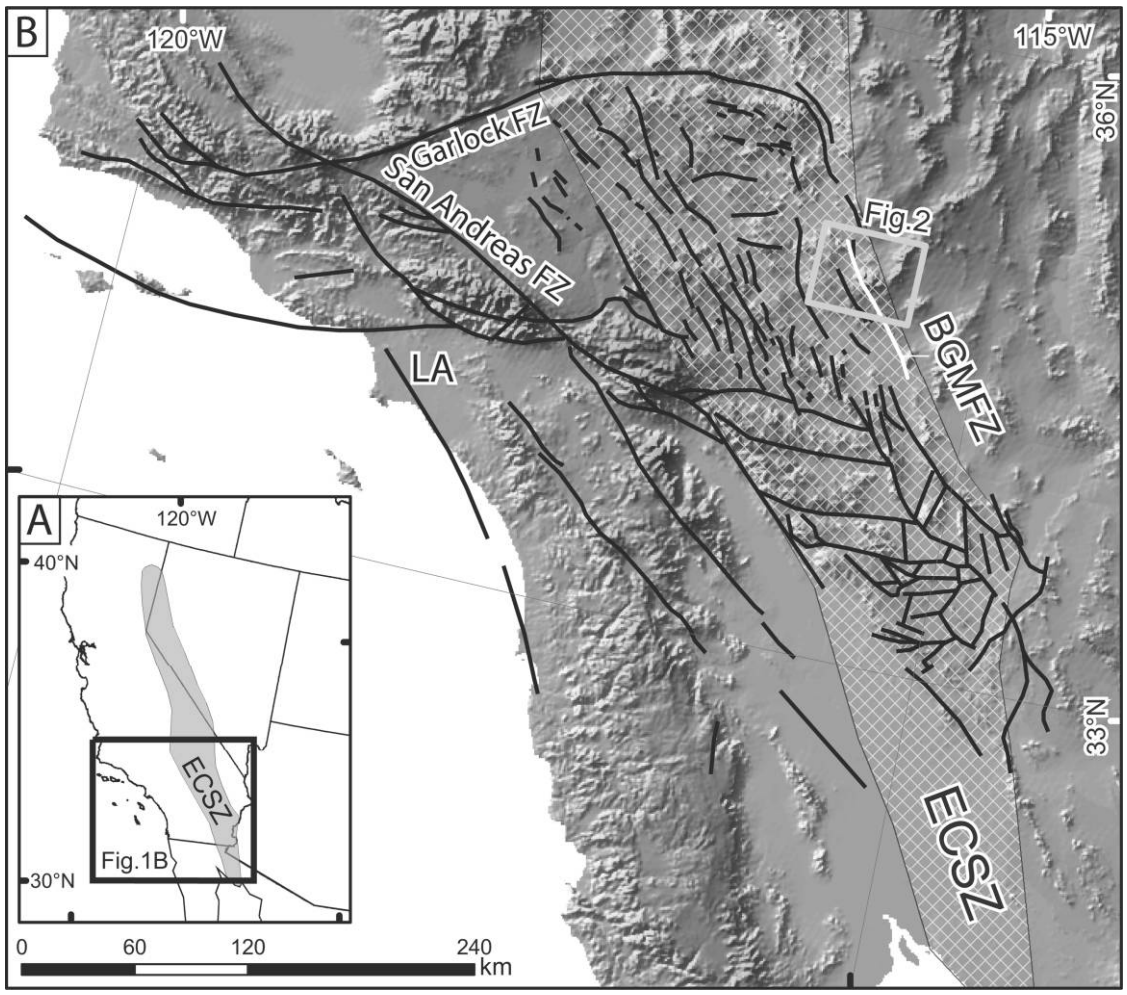

Figure 1. *A*, Location map. *B*, Faults within the southern Eastern California Shear Zone (*ECSZ*; cross-hatched). *LA* = Los Angeles, *BGMFZ* = Bristol-Granite mountains fault zone. The Mojave Block is bounded by the *BGMFZ*, the *San Andreas fault zone* (*FZ*), and the *Garlock FZ*. The area of figure 2 is outlined.

The southern ECSZ is composed of a ~100-km-wide network of late Neogene and Quaternary strike-slip faults that extend from the Gulf of California north through the Mojave Desert (fig. 1). The northwest-striking dextral faults define the structural grain of a series of linear, fault-bounded ranges. Initiation of dextral faulting and related rotation of fault blocks in the northeast Mojave Desert and eastern Transverse Ranges occurred in the middle to late Miocene, though the exact timing is poorly defined. Before dextral faulting, much of the southern ECSZ was host to early Miocene (22–18.5-Ma) northeast-directed extension (Dokka and Travis 1990*a*; Walker et al. 1990; Brady 1993; Miller 1993; Glazner et al. 2002; McQuarrie and Wernicke 2005).

North of the Garlock Fault, the ECSZ continues with the northwest-trending, subparallel Death Valley–Furnace Creek, Fish Lake Valley, and White Mountains–Owens Valley fault zones (e.g., Stewart 1988; Lee et al. 2005). The ECSZ steps east at the Mina deflection and dextral shear continues along the Walker Lane fault belt of west-central Nevada, with some residual plate motion transferred into the central Nevada seismic belt (Oldow 1992; Oldow et al. 2001).

Dextral shear in the Mojave portion of the ECSZ should be kinematically linked to tectonism in surrounding regions, which includes rotation of the eastern transverse ranges from 10 to 4 Ma (Carter et al. 1987; Richard 1993), extension and shear north of the Garlock fault between 11 and 3 Ma (Snow and Lux 1999; Snow and Wernicke 2000; Niemi et al. 2001), and the northwesterly motion of the Sierra Nevada–Great Valley block (Wernicke and Snow 1998; McQuarrie and Wernicke 2005). The left-lateral Garlock fault acts as a continental transform by separating large magnitudes of oblique extension in the north from dextral shear and contraction in the ECSZ to the south (Davis and Burchfiel 1973; Bartley et al. 1990). Because the geologic record north and south of the Garlock fault does not permit any structural overlap of these two regions, reconstructions of the ECSZ system mandate equal magnitudes of dextral displacement in both regions (McQuarrie and Wernicke 2005). A proposed displacement for the ECSZ system based strongly on geological offsets north of the Garlock fault suggests 100 ± 10 km of dextral shear oriented N25W between 12 and 0 Ma (McQuarrie and Wernicke 2005). However, field studies throughout the Mojave block have documented only 53 ± 6 km of dextral shear (Glazner et al. 2002). Whereas some structures have well-constrained, documented offsets (Dibblee 1961; Garfunkel 1974; Dokka 1983; Oskin and Iriondo 2004), others are poorly constrained and potentially could provide some of the missing dextral shear.

Previous Estimates of Slip Magnitude across the BGMFZ. The BGMFZ (Gamble 1959*a*, 1959*b*) is the easternmost fault within the Mojave portion of the ECSZ and separates the neotectonically active Mojave block (to the west) from the relatively stable Sonoran block (to the east). The BGMFZ is a network of vertical strike-slip faults that extends >75 km along the entire length of the Bristol, Granite, Old Dad, and Marble mountains, contributing to the northwest-southeast structural grain of these ranges. In the region between the Old Dad and Granite mountains, the BGMFZ is as narrow as a few hundred meters and is covered by alluvium of the modern Budweiser Wash. Here, the fault dips 70°–80° northeast, and steep gravity gradients indicate that it is a major structure that places Mesozoic granitoid rocks adjacent to Tertiary volcanic rocks (Howard et al. 1987; Hendricks 2003).

Available geologic estimates of cumulative dextral offset along the BGMFZ (0–15 km) are either highly debated or not tightly constrained (fig. 2; table 1; Brady 1992, 1993; Howard and Miller 1992). On the other hand, reconstruction estimates based on regional kinematic compatibility (i.e., slips on unconstrained faults are adjusted to eliminate geologically unexplained overlaps or gaps) suggest relatively large (21–27 km) magnitudes of dextral offset along the BGMFZ (Dokka and Travis 1990*a*; McQuarrie and Wernicke 2005).

Dokka and Travis (1990*a*) proposed 21.5 km of dextral offset across the BGMFZ based on a kinematic model of strain compatibility; this restoration allows similar Mesozoic basement rocks and middle Tertiary volcanic rocks to align in the vicinity of the Granite, Marble, and Bristol mountains (fig. 2; table 1). However, mapping reported by Howard and Miller (1992) indicated that the basement plutons are of diverse types and different ages, ranging from Cretaceous to Proterozoic, and are therefore noncorrelative. Howard and Miller (1992) alternatively proposed 0–10 km of BGMFZ offset based on an east-trending outcrop pattern of lower Miocene, flow-banded rhyolite lava (Miller 1993). The rhyolite crops out on opposite sides of the fault in the Van Winkle Mountains and the Bristol Mountains with perhaps minor offset. Mapping proximal to the BGMFZ in the Old Dad and northern Marble mountains indicates that flow-banded rhyolite is not a unique marker in this region, compromising its utility in measuring dextral offset across the BGMFZ.

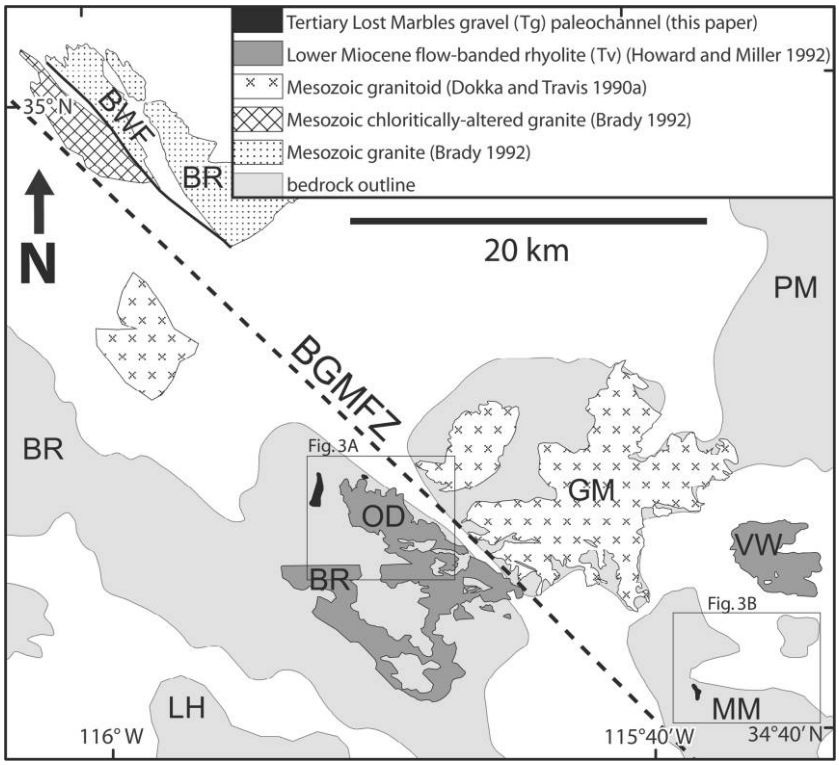

Figure 2. Different lithologic markers correlated across the Bristol-Granite mountains fault zone (*BGMFZ*). See table 1 for offset estimates. *BR* = Bristol Mountains, *BWF* = Balch Wash Fault, *GM* = Granite Mountains, *LH* = Lava Hills, *MM* = Marble Mountains, *OD* = Old Dad Mountains, *PM* = Providence Mountains, *VW* = Van Winkle Mountain. The areas of figures 3*A*, 3*B* are outlined.

Brady (1993) suggested that the close connection between bedrock types and sediment provenance in the northern Bristol Mountains indicates that dextral offset along any one strand of the BGMFZ does not exceed the 15-km length of the range, though cumulative BGMFZ offset may be greater. Additionally, the Balch Wash fault dextral offset estimate of >6 km (Brady 1992) is for an individual fault strand and does not provide an upper bound for total offset across the fault zone as a whole.

Field mapping of the Old Dad and northern Marble mountains was completed at 1 : 24, 000 scale (fig. 3; table 2) to test whether the 27-km BGMFZ offset estimate provided by regional reconstructions (McQuarrie and Wernicke 2005) is validated by a geologic piercing point proximal to the BGMFZ.

Table 1. Estimates of Dextral Offset across the Bristol Granite Mountains Fault Zone

Dextral offset (km)	Location	Data used	Reference
21.5	Mojave Block	Cenozoic regional reconstructions; alignment of Mesozoic basement rocks and Tertiary volcanic rocks	Dokka and Travis 1990*a*
0–10	Bristol and Van Winkle mountains	Alignment of Tertiary rhyolite flows and metavolcanic rocks	Howard and Miller 1992
>6	Northern Bristol Mountains, Balch Wash fault segment	Juxtaposition of fresh Mesozoic granite against chloritically altered Mesozoic granite	Brady 1992
<15	Northern Bristol Mountains	Tertiary sedimentary clast provenance	Brady 1993
27	Southwestern North America	Cenozoic regional reconstructions	McQuarrie and Wernicke 2005
24+	Old Dad and Marble mountains	Alignment of Tertiary paleovalley	This article

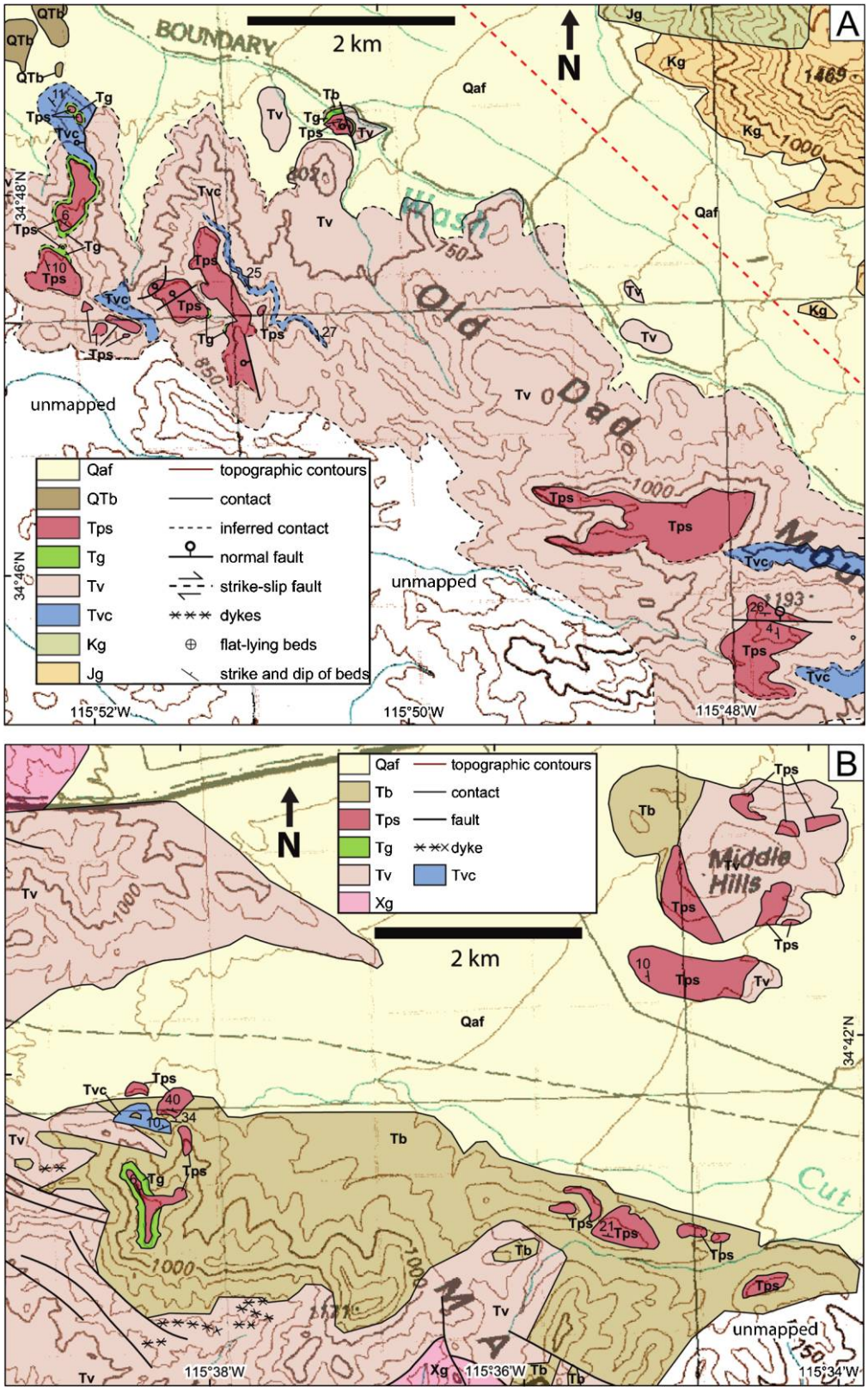

Figure 3. *A*, Geology of the northern Old Dad Mountains, California (map data from Miller et al. 2003 and our own data). See table 2 for description of map units. *B*, Geology of the northern Marble Mountains, California (map data from Glazner and Bartley 1990, Miller et al. 2003, and our own data).

Table 2. Mapped Units

Symbol	Unit (age)	Description
Qaf	Alluvial fan deposits and alluvium (Holocene and Pleistocene)	Unconsolidated deposits of poorly sorted gravel, sand, and silt deposited as alluvial cones at mouths of canyons and gullies, as alluvial floodplains that border streams, and as braided-stream sediments in stream channels; older deposits form piedmonts that flank mountain ranges, as well as typically underlie raised, paved, and varnished surfaces; mapped by Miller et al. (2003)
QTb	Basalt (Quaternary and Tertiary)	Basalt flows of northern Old Dad Mountains
Tps	Peach Springs Tuff (middle Miocene)	Widely distributed rhyolite ash-flow tuff that contains adularescent blue sanidine, ubiquitous but minor amounts of sphene, and variable amounts of biotite and hornblende; basal layer 1 is white to light gray and composed of pumice, coarse ash, and small lapilli commonly bedded and cross-bedded; middle layer 2a is tan to orange and partially welded/nonwelded, and it contains basal pumice and lithic fragments; upper layer 2b is gray to mauve, vapor-phase devitrified, and has erosional caverns, sheet joints, and vertical joints (Valentine et al. 1989); age is 18.5 ± 0.2 Ma (Nielson et al. 1990)
Tg	Lost Marble gravel (middle Miocene)	Localized slope-forming unit composed of highly-rounded cobbles of intermediate to mafic volcanic rock that are typically covered by angular talus of the Tps unit
Tv	Volcanic rocks (early Miocene)	Rhyolite lava flows and ash flows, tuffaceous sedimentary rocks, tuff breccia, basalt flows, and andesite flows
Tvc	Volcaniclastic rocks (early Miocene)	Tuffaceous sedimentary rocks intercalated within the Tv unit
Tb	Castle basalt (early Miocene)	Basalt and basltic andesite flows with locally scoriaceous tops (Glazner and Bartley 1990)
Kg	Granodiorite and porphyritic monzogranite (Cretaceous)	Equigranular hornblende-biotite granodiorite intruded by light-gray, coarse-grained biotite monzogranite that contains K-feldspar phenocrysts; units Kgd and Kpm of Miller et al. (2003)
Jg	Quartz diorite gneiss, diorite, and granitoid rocks (Jurassic)	Hornblende quartz diorite and quartz monzodiorite that contains megacrysts of K-feldspar and has a ~160-Ma age (unit Jqd of Miller et al. [2003]); dark brown to black hornblende diorite, hornblende-biotite monzodiorite, and mafic porphyritic hornblende-biotite quartz monzonite (unit Jd of Miller et al. [2003]); hornblende-biotite granodiorite, porphyritic granite and alkali granite, biotite-hornblende monzodiorite, and related rocks (unit Jg of Miller et al. [2003]); K-feldspar phenocrysts in porphyritic granitoids are typically pink or purple
Xg	Granitoid rocks (Early Proterozoic)	Granite, granodiorite, and diorite dated at between 1660 and 1695 Ma (Wooden and Miller 1990); common rock types are strongly porphyritic biotite granite, inequigranular leucocratic granite, and hornblende-biotite granodiorite; locally foliated; mapped by Miller et al. (2003)

Early Miocene Stratigraphy of the Old Dad and Marble Mountains

Lost Marble Gravel. Detailed mapping of volcanic and volcaniclastic rocks within the northern Old Dad and northern Marble mountains revealed distinctive alluvial gravel deposits (fig. 4*B*, 4*C*) that are preserved directly beneath a few mesa-forming outcrops (fig. 4) of the 18.5 ± 0.2-Ma Peach Springs Tuff, a regionally extensive ash flow tuff (Glazner et al. 1986; Nielson et al. 1990). The gravel was observed only in the northernmost portions of each range. Other outcrops of the Peach Springs Tuff are devoid of underlying gravel (fig. 3). The restricted area of gravel deposits in both ranges and the similarity among gravel outcrops make the gravel an appealing candidate to constrain right-lateral offset along the BGMFZ. The distinctive gravel deposits are herein informally termed the "Lost Marble" gravel, after sites 1A–1C (fig. 5*B*), the thickest and most extensive gravel exposure found in the northern Marble Mountains (fig. 4*A*, 4*B*).

The Lost Marble gravel is composed of well-sorted, clast-supported, pebble to cobble conglomerate beds (fig. 4*B*). Exposures of this unit tend to be poor and require trenching, but where exposed, the clasts are stratified and beds contain evidence of weakly to moderately developed imbrication. At site 1A, the deposits show evidence of crude stratification and exhibit an upward-fining trend in a few

layers with clasts of cobble- and boulder-sized material at the base of an individual bed grading into pebble-sized material at the top. Individual clasts are typically well-rounded to very well-rounded and spherical to slightly oblate. Clasts are almost exclusively volcanic, with dacitic to basaltic compositions (fig. 6*A*). Basaltic clasts are commonly very fine-grained and vesicular (including clasts of scoria), in rare instances containing visible olivine and plagioclase phenocrysts; dacite and andesite clasts are more varied but typically contain abundant plagioclase. Also present are rare clasts of tuffs and tuffaceous volcaniclastic rock. Only one clast with granitic characteristics was observed out of the 190 clasts counted.

The Lost Marble gravel underlies only select Peach Springs Tuff exposures (sites 1, 3, and 4) in the northern portions of the Old Dad and Marble mountains. Gravel thicknesses were inferred (figs. 5, 7) based on the interval between the better-exposed, more resistant units above the gravel (Peach Springs Tuff) and below (Tertiary basalt, andesite, or volcaniclastics) because of the recessive weathering nature of the Lost Marble gravel deposits (e.g., fig. 4*A*, 4*C*). The Lost Marble gravel is 20 m thick at site 1 and 8 m thick at sites 3 and 4 (figs. 5, 7).

The Lost Marble gravel is interpreted as a coarse-grained fluvial deposit. The mature texture of the individual clasts, their imbrication, and well-defined stratification are most consistent with transport by fluid, flow-related traction currents (Nemec and Steele 1984; Miall 1996). The compositions of individual clasts are most similar to underlying Tertiary volcanic units exposed in selected areas of the Mojave Desert (Miller et al. 2003), and there is a striking absence of granitic clasts despite the widespread exposure of granite in the nearby Granite Mountains (fig. 2). The well-sorted nature of the clasts, their textural maturity, and the absence of any angular material suggests that the Lost Marble gravel was transported from distal sources. Paleocurrent directions were difficult to determine because of the poor exposures. Clast imbrications show considerable scatter (fig. 6*B*) and are thus inconclusive.

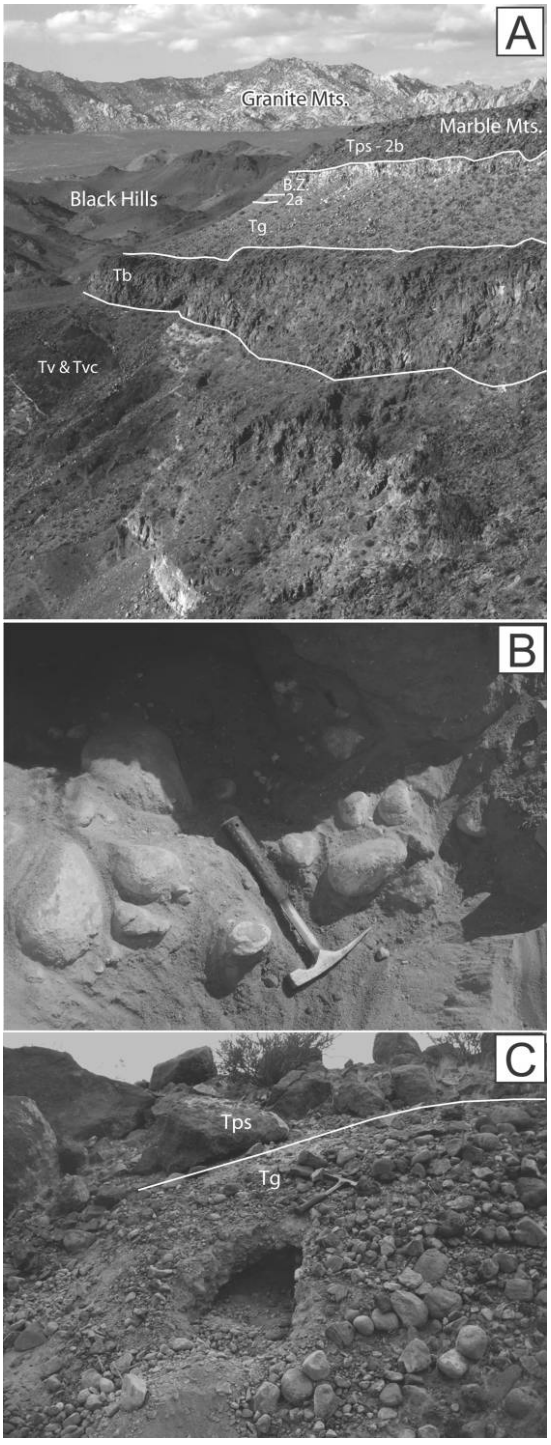

Figure 4. *A*, Top to bottom: mesa capped by Tertiary Peach Springs Tuff (*Tps*, further subdivided into units *2B*, *B.Z.*, *2A*), underlain by slope-forming Lost Marble gravel (*Tg*), underlain by ledge-forming scoriaceous top of the Castle basalt (*Tb*), which is underlain by volcanics (*Tv*) and volcaniclastics (*Tvc*). Granite Mountains and Black Hills in background to north. Photo shows sites 1A and 1B in the northern Marble Mountains. *B*, Lost Marble gravel outcrop showing well-rounded, clast-supported, well-sorted cobble gravel. Photo taken at site 1A in the northern Marble Mountains. *C*, Contact between Lost Marble gravel and Peach Springs Tuff lag deposit. Photo taken at site 3A in the northern Old Dad Mountains.

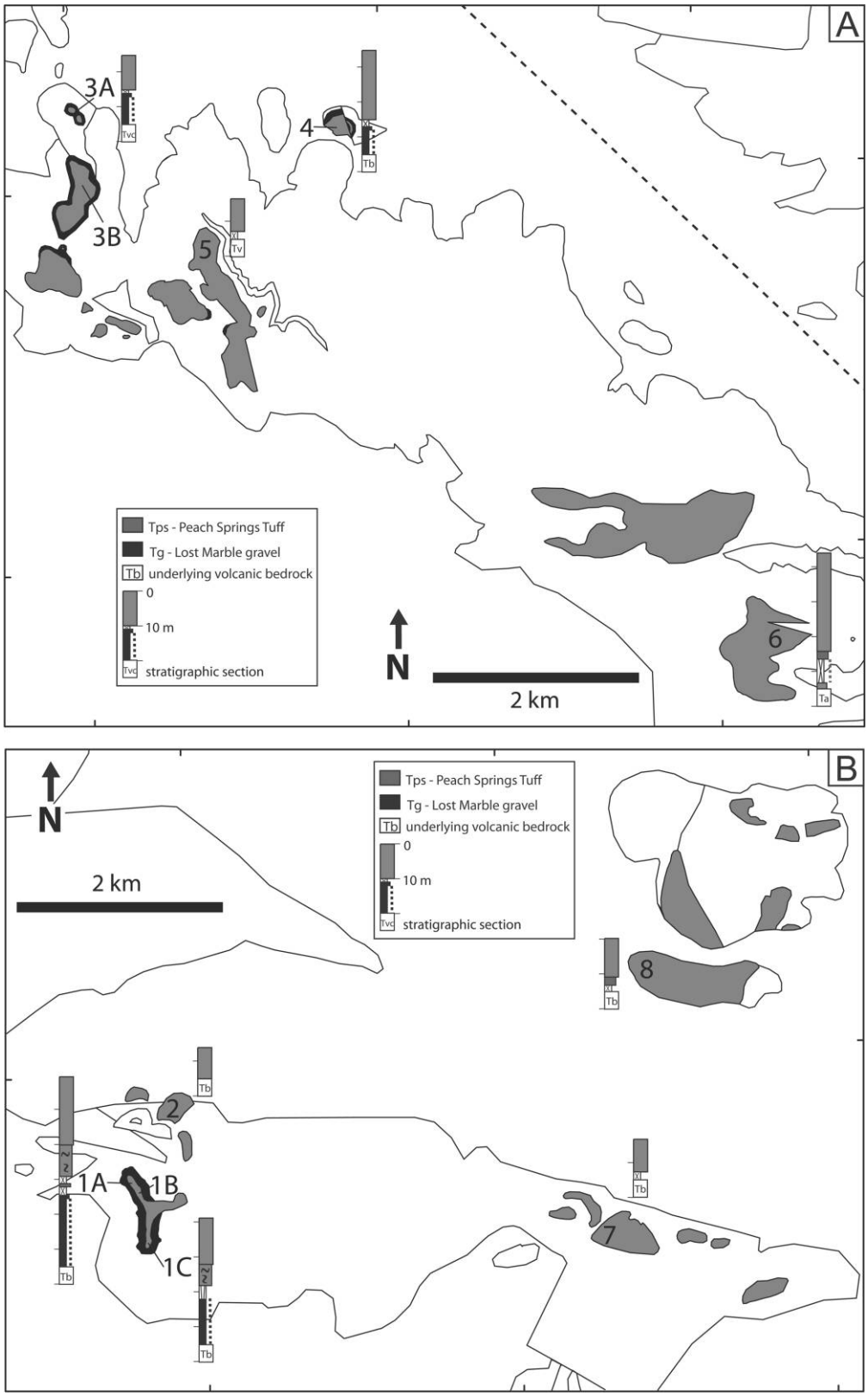

Figure 5. Site locations and measured stratigraphic sections (see fig. 7 for more details) in the Old Dad Mountains (*A*) and Marble Mountains (*B*). Locations of figure 5*A* and 5*B* are identical to locations of figure 3*A* and 3*B*, respectively.

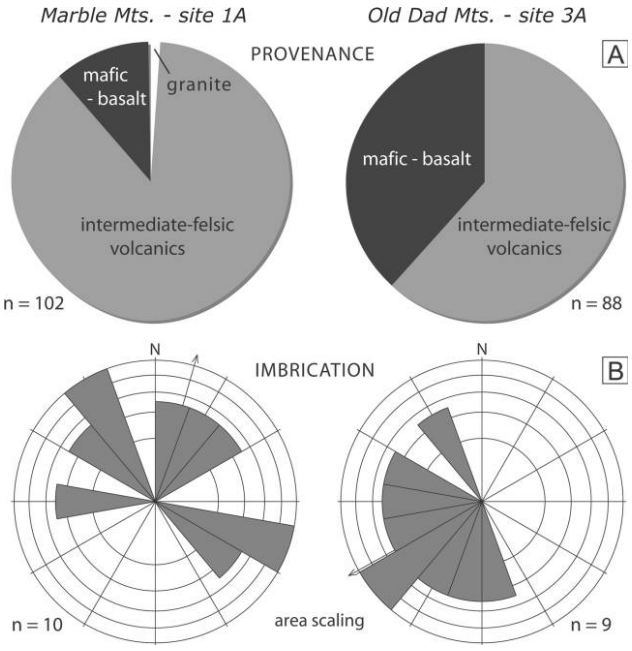

Figure 6. Lost Marble gravel provenance (*A*) and imbrications (*B*) showing inferred paleocurrent direction from the Old Dad and Marble mountains. Intermediate-felsic volcanics include andesite and dacite. $n =$ number of imbricated clasts measured at site.

Peach Springs Tuff. The Peach Springs Tuff is a rhyolitic, welded ignimbrite that crops out in scattered locations over an area greater than $32,000$ km^2 covering the triple juncture of Nevada, California, and Arizona (Buesch 1993). The tuff represents a single cooling unit (Young and Brennan 1974), with the majority of the formation deposited by a single, high-volume, relatively continuously discharging pyroclastic flow (Valentine et al. 1989). It has been dated at 18.5 ± 0.2 Ma (Nielson et al. 1990). The tuff dispersed in a series of arms (interpreted to be infilled paleovalleys) radiating from a possible source near the southern tip of Nevada (Buesch 1989; Hillhouse and Wells 1991). A ~25-km-wide E-W-trending zone of tuff outcrops extends into the Mojave Desert and appears to have been displaced progressively northward along a series of right-lateral faults (Wells and Hillhouse 1989).

The Peach Springs Tuff is subdivided into layer 1, a basal layered deposit, and layer 2, a massive pyroclastic flow deposit (table 2; fig. 7; Valentine et al. 1989). Layer 1 deposits are white to light gray and composed of pumice, coarse ash, and small lapilli, and they are commonly bedded and cross bedded. Layer 2 deposits are light gray to mauve and welded, and they contain distinctive adularescent blue sanidine phenocrysts. The layer 2 phenocryst assemblage is sanidine ≫ plagioclase ± quartz, with hornblende > biotite ± clinopyroxene and magnetite ± ilmenite (Buesch 1993). The upper portion of layer 2 (2b) is gray to mauve and vapor-phase devitrified, and it has erosional caverns, sheet joints, and vertical joints. The lower portion of layer 2 (2a) is tan to orange and partially welded/nonwelded and contains basal pumice and lithic fragments. Outcrops in Kingman, Arizona, ~30 km from the proposed vent area, have layer 2 deposits ~75 m thick where they are observed along the axial portions of paleovalleys and ~25 m thick where observed along paleovalley margins or other paleogeographic highs.

Mesa-capping tuff outcrops in our study area (fig. 3) have been identified by us and others as Peach Springs Tuff, based on their distinctive phenocryst assemblage and geochemistry, remanent magnetism, and K-Ar ages (Wells and Hillhouse 1989; Nielson et al. 1990; Buesch 1993). Peach Springs Tuff found in the Bristol, Old Dad, and Marble mountains has phenocrysts of blue adularescent sanidine and hornblende visible in hand samples, with minor amounts of magnetite and sphene, which is a phenocryst assemblage unique for Mojave region tuffs (Glazner et al. 1986). Furthermore, phenocryst geochemistry from sites that include the Bristol and Marble mountains shows that the Peach Spring tuff is distinct from other Miocene regional tephra units, particularly when comparing sanidine end members (Buesch

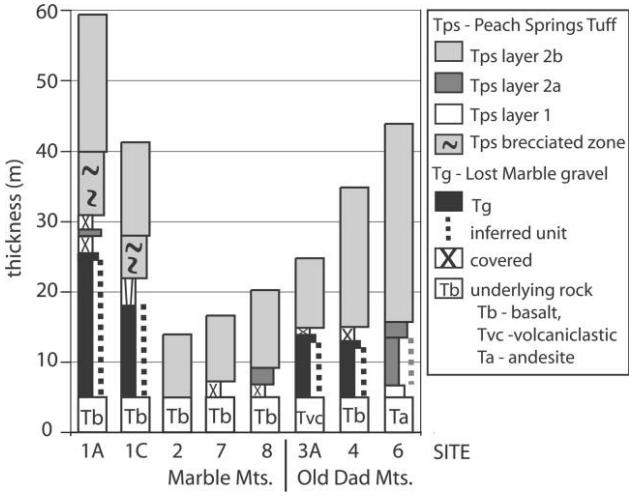

Figure 7. Measured stratigraphic sections of the Lost Marble gravel and the Peach Springs Tuff from sites in the Old Dad and Marble mountains. See figure 5 for locations.

1993). Also, tuffs identified as Peach Springs Tuff that were sampled for paleomagnetism in the Bristol and Marble mountains and other sites show a thermoremanent paleomagnetic direction (~33° declination, ~36° inclination) that distinguish its direction of magnetization from the usual range of secular variation (Wells and Hillhouse 1989). The Peach Springs Tuff has proven difficult to date precisely. Samples of the Peach Springs Tuff from the Bristol and Marble mountains yielded K-Ar ages of ~16–20 Ma, broadly consistent with a 18.5 ± 0.2-Ma Ar-Ar age of the tuff (Nielson et al. 1990).

Peach Springs Tuff exposed along the BGMFZ is ~85–115 km away from the proposed vent area, which was identified based on tuff thickness, outcrop pattern, and flow direction deduced from magnetic anisotropy (Buesch 1989; Hillhouse and Wells 1991). In the Old Dad Mountains, the tuff thickens southward, increasing from 10 m at site 3a to 40 m thick at site 6 (figs. 5, 7). In the northern Marble Mountains, the tuff thickens to the southwest, increasing from 10 m thick at site 2 to 30 m thick at site 1a and 20 m thick at site 1c. Layer 2b is found at all measured section sites, whereas the less resistant layers 2a and 1 are exposed only at certain sites.

Anisotropy of Magnetic Susceptibility (AMS)—Peach Springs Tuff

AMS has been successfully employed to determine the flow direction of ash-flow tuffs (Ellwood 1982; MacDonald and Palmer 1990, 1991; Hinz et al. 2009) because AMS reflects the orientation of titanomagnetite grains during ignimbrite emplacement (Hrouda 1982). Flow direction is often intimately linked to topography because local features (i.e., valleys) will channelize ash-flow. Thus AMS measurements have been used to infer the orientations of paleovalley segments (Hinz et al. 2009). We collected AMS data from 10 sites in the vicinity of the BGMFZ (fig. 5) to document the direction of Peach Springs Tuff paleoflow on both sides of the fault, particularly in areas underlain by the Lost Marble gravel. This investigation was undertaken to better constrain the orientation of the paleovalley in which the gravel was deposited. A previous paleomagnetic investigation of the Peach Springs Tuff regional paleoflow gave good quality AMS data (Hillhouse and Wells 1991).

The magnetic susceptibility (k) of a specimen relates its induced magnetic moment (M) to the external applied field (H) through the equation $M = kH$. Anisotropy of magnetic susceptibility (AMS) describes the directional dependence of magnetic susceptibility and is expressed as a triaxial ellipsoid, with K1 being the maximum susceptibility direction, K2 the intermediate direction, and K3 the minimum direction. In general, ignimbrites have a weak anisotropy (1%–3%), owing to the preferred shape alignment of nearly equidimensional magnetite or maghemite grains. Two fabric elements are used to describe the AMS of ignimbrites: K1 defines the magnetic lineation, and K3 defines the pole to the magnetic foliation/imbrication. AMS K1 and K3 directions were determined, and their associated 95% confidence fans were constructed for each of several sites in the Old Dad and Marble mountains and then compared with results from an earlier, regional AMS study of the Peach Springs Tuff (figs. 8, 9; Hillhouse and Wells 1991). Unfortunately, these data proved largely inconclusive for precisely defining the orientation of the paleovalley that hosted the Lost Marble gravel. See the appendix, available in the online edition or from the *Journal of Geology* office, for additional information concerning AMS methods.

Discussion

Lost Marble Paleovalley. We propose that the Lost Marble gravel deposits define a pre-18.5-Ma paleovalley, based on their remarkably similar clast size, provenance, texture, stratigraphic position (underlying a tuff marker horizon), and outcrop thicknesses, as well as the restricted area of gravel deposits in both the Old Dad and Marble mountains. Within the ~25 km wide, east-west trending belt of Peach Springs Tuff outcrops in the Mojave region, the restricted series of Lost Marble gravel outcrops delimit a narrower paleovalley that has since been offset by the BGMFZ.

Pre-18.5-Ma dip-slip faulting on the BGMFZ is supported by different exposure levels in the Peach Springs Tuff subcrop (Howard et al. 1987). The combination of deeper Mesozoic plutonic exposure levels on the east side of the fault and an unknown thickness section of Miocene volcanic rocks on the Old Dad (west) side of the fault suggests that before the dextral offset, the Granite Mountains were elevated relative to the Old Dad Mountains. Given this dip-slip, it is likely that the Granite Mountains never had a significant Miocene volcanic cover comparable to the volcanic cover seen in the Old Dad and Marble mountains. The late Tertiary Bull Canyon normal fault, which defines the northwestern margin of the Granite Mountains, helped expose plutonic rocks in the footwall of the Granite Mountains (Howard et al. 1987).

If significant accommodation space existed in the downthrown block of the Old Dad Mountains, then gravel outcrops there should be extensive and covered with a sheet of Peach Springs Tuff. However, gravel deposits are thin and localized on both sides of the BGMFZ, indicating either little dip-slip on the BGMFZ immediately pre-18.5 Ma or that the accommodation space created by pre-18.5-Ma BGMFZ dip-slip was filled by Miocene volcanic rocks before the eruption of the Peach Springs Tuff. Thus, most of the region was exposed at 18.5 Ma, and the paleovalley appears to be confined on both sides of the fault.

Geologic Constraints on Paleovalley Orientation. Reconstruction of the Lost Marble paleovalley orientation provides an estimate of BGMFZ offset. We propose the map pattern of Peach Springs Tuff outcrops underlain by Lost Marble gravel and those tuff outcrops devoid of underlying gravel delineate the margins of the paleovalley on either side of the fault as well as define the paleovalley orientation. In the Old Dad Mountains, the outcrop pattern indicates that the southern margin of the paleovalley lies between sites 3A, 3B, and 4 (gravel), and site 5 (no gravel) and has a west-southwest orientation (fig. 10). In the Marble Mountains, the northern margin of the paleovalley lies between sites 1A, 1B, and 1C (gravel) and sites 2, 7, 8 (no gravel) and has a west-northwest orientation. More uncertain are the northern paleovalley margin in the Old Dad Mountains and the southern margin in the Marble Mountains; in the Old Dad Mountains, the northern paleovalley margin lies north of site 3a, and in the Marble Mountains, the southern paleovalley margin lies south of site 1c.

The provenance of Lost Marble gravel clasts (fig. 6*A*) provides an additional constraint on the orientation of the paleovalley. The absence of granitic clasts in the Old Dad and Marble mountains implies that the Lost Marble paleovalley did not incorporate clasts from the nearby, paleotopographically high Granite Mountains. Thus, northwest and northeast paleovalley orientations that cross the Granite Mountains are excluded.

The Peach Springs Tuff thickens southwards in both the Old Dad and Marble mountains. However, using the apparent variations in preserved Peach Springs Tuff thickness to map out the paleovalley is problematic because different sites have different

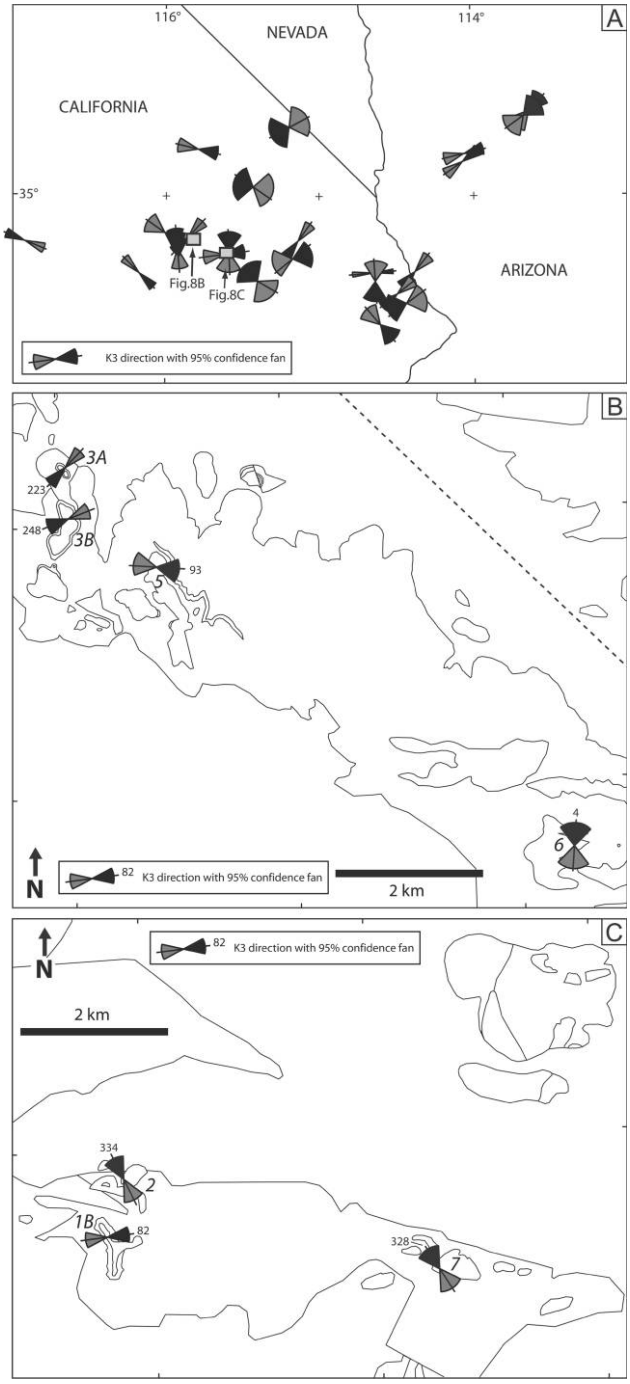

Figure 8. Map distribution of K3 directions and associated 95% confidence fans for Peach Springs Tuff anisotropy of magnetic susceptibility (AMS) sites across the entire ignimbrite sheet (*A*; Hillhouse and Wells 1991), in the Old Dad Mountains (*B*), and in the Marble Mountains (*C*). Blackened fan indicates plunge direction. In *B*, note the consistent southwest K3 direction for the two northern sites, both of which are underlain by Tg. In *C*, note the east-west K3 direction for site 1B, which is underlain by Tg, and the northwest K3 direction for other sites. Locations of *B* and *C* are identical to the locations of figure 3*A* and 3*B*, respectively. See the appendix, available online or from the *Journal of Geology* office, for additional information concerning AMS methods.

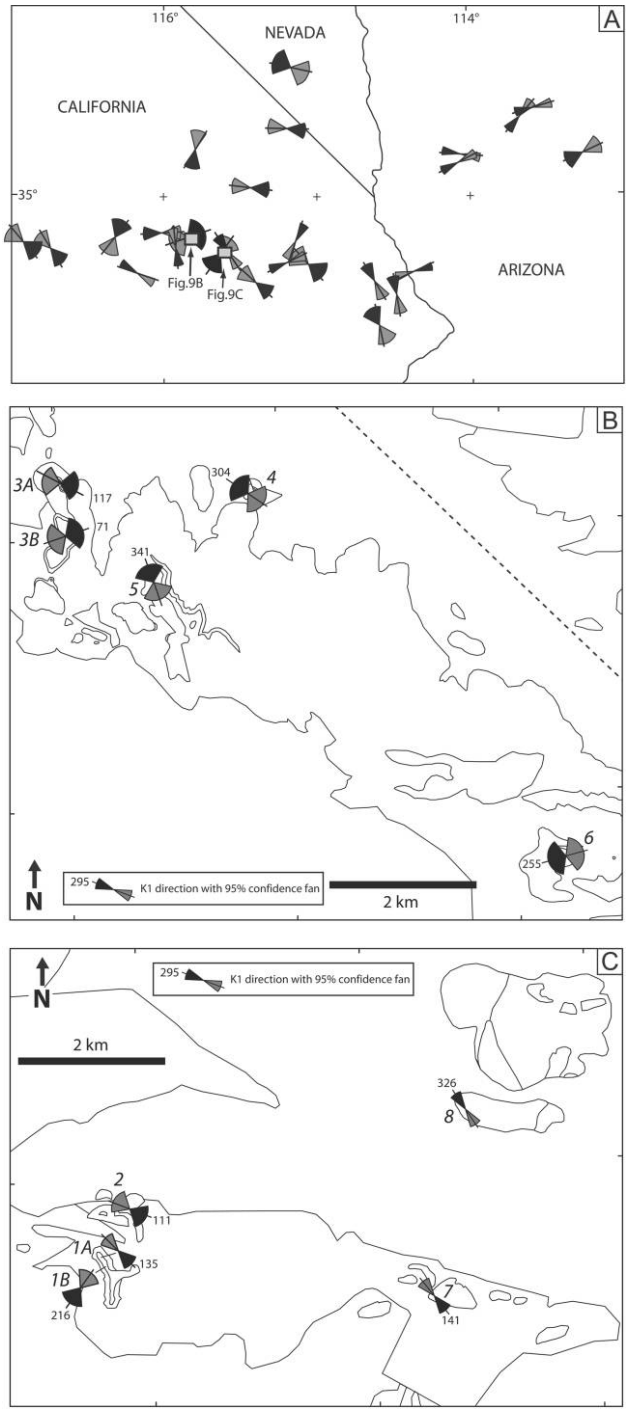

Figure 9. Map distribution of K1 directions and associated 95% confidence fans for Peach Springs Tuff anisotropy of magnetic susceptibility sites across the entire ignimbrite sheet (*A*; Hillhouse and Wells 1991), in the Old Dad Mountains (*B*), and in the Marble Mountains (*C*). Blackened fan indicates plunge direction. In *B*, note the large 95% confidence fans and scatter of directions, and in *C*, note the generally consistent southeast K1 direction. Locations of *B* and *C* are identical to the locations of figure 3*A* and 3*B*, respectively.

lithologic characteristics, casting uncertainty on whether the preserved tuff thickness reflects the original depositional thickness for each individual site. Postdepositional erosional stripping of the upper partially welded or nonwelded portions of the Peach Springs Tuff is common locally (Buesch 1991). Given this site-specific uncertainty, we do not give much weight to comparing tuff isopachs on either side of the fault as a means of constraining offset.

AMS and Tuff Paleoflow. The gravel that defines the Lost Marble paleovalley is everywhere overlain by Peach Springs Tuff, and thus, assuming tuff flow is intimately linked to topography, tuff paleoflow may be used to independently assess the orientation of the paleovalley. An earlier, regional study of the Peach Springs Tuff defined the principal AMS directions and magnitudes for 41 sites from the entire ignimbrite sheet (Hillhouse and Wells 1991). From the proposed Peach Springs Tuff vent near the southern tip of Nevada, the tuff flowed to the southwest into the Mojave Block with locally turbulent conditions (figs. 8*A*, 9*A*). Our AMS study complements existing data by focusing on a denser array of sites in close proximity to the BGMFZ and targeting tuff sites directly overlying the Lost Marble gravel. An AMS sample locality common to both studies in the Middle Hills (site 8 of this study and site 32 of Hillhouse and Wells [1991]) shows reasonable agreement with K1 and K3 declinations differing by <30°

The standard magnetic fabric for clastic rocks predicts a lower-hemisphere AMS K3 (pole to foliation) oriented in the flow direction and a lower-hemisphere K1 (lineation) that is oriented parallel but opposite in sense to the flow direction (Rees 1968), which holds for some ignimbrites (e.g., Macdonald and Palmer 1990; Palmer et al. 1991, 1996). However, K1 is not always distinguishable from K2; sometimes, K1 and K2 are identical in magnitude and K1 and K2 directions from multiple cores collected at the same site define a girdle indicating a magnetic foliation/imbrication. In these cases, K3 best characterizes the flow direction (e.g., Cagnoli and Tarling 1997; Le Pennec et al. 1998) since the uniqueness of K1 is ambiguous. For Peach Springs Tuff sites underlain by the Lost Marble gravel in the Old Dad and Marble mountains, K3 appears to be a more reliable and consistent bidirectional magnetic direction than K1.

A K1 + K2 imbrication plane (with a K3 pole) is strongly suggested for several sites (1B, 3A, 3B, 4, 5, and 6; see figs. A1, A2, available online or from the *Journal of Geology* office) by overlapping K1 and K2 directions, bootstrapped directions, and eigenvalues

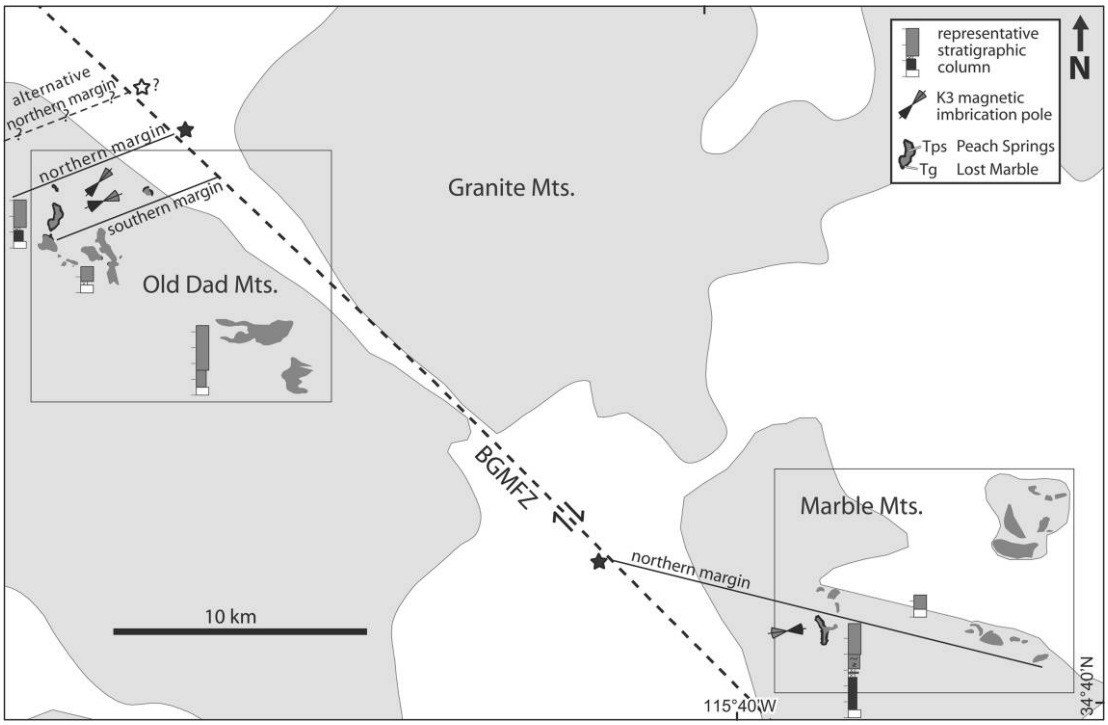

Figure 10. Geological and selected anisotropy of magnetic susceptibility data bearing on the existence and orientation of the Lost Marble paleovalley. Piercing point correlation of the northern margin of the paleovalley (*star*) indicates a minimum of 24 km of dextral offset along the Bristol-Granite mountains fault zone (BGMFZ). Boxed areas indicate identical locations of figures 3*A* and 3*B*, 5*A* and 5*B*, 8*B* and 8*C*, and 9*B* and 9*C*, respectively, in the Old Dad Mountains and the northern Marble Mountains.

that indicate that K1 and K2 are indistinguishable. Furthermore, large K1 95% confidence ellipses ($E12 > 45$) suggest that a principal component analysis does not characterize the distribution any better than a uniform distribution (Mark 1973). Paleoflow using K3 is generally consistent for Peach Springs Tuff sites that overlie the Lost Marble gravel. These sites together have a coherent bidirectional K3 imbrication direction that suggests west-southwest paleoflow. Specifically, Old Dad Mountains sites 3A and 3B suggest southwest flow, whereas Marble Mountains site 1B suggests west bidirectional paleoflow (fig. 8). The K1 and K3 direction are in general agreement for site 3B, as expected from the standard magnetic fabric for clastic rocks.

In contrast to the consistent AMS K3 directions for Peach Springs Tuff sites overlying the Lost Marble gravel, those tuff sites devoid of underlying gravel indicate a variety of flow directions. East flow (site 5; fig. 8) and north flow (site 6) are suggested for Old Dad Mountains sites where K3 best describes the flow direction. Northwest flow is suggested (sites 1A, 2, 7, 8; fig. 9) for Marble Mountains sites where K1 may best describe flow direction. Furthermore, relatively shallow K3 inclination at several sites may suggest ramping at the flow margin and locally turbulent flow.

The AMS results have several caveats. Poor separation of the K1 and K2 directions may be the result of two main factors: (1) the Peach Springs Tuff magnetic fabric is intrinsically subtle in the plane of flow, and/or (2) the number of specimens used to determine AMS was low, leading to large/overlapping confidence limits. Additionally, tuff flow directions inferred from near-vertical K3 directions are especially prone to error induced by relatively small errors in the tilt correction. It is also worth noting that we expect no significant vertical axis rotations of fault-bounded blocks in our study area, based on a previous investigation of the Peach Springs Tuff (Wells and Hillhouse 1989). Remanent magnetization directions from localities in the Bristol Mountains (immediately west of the Old Dad Mountains) and Middle Hills (immediately east of the Marble Mountains) suggest $<5°$ rotations rela-

tive to the stable Colorado Plateau, though overlapping 95% confidence intervals suggest that no rotation is statistically distinguishable.

In summary, paleoflow using K3 is generally consistent for tuff sites that overlie the Lost Marble gravel, whereas other tuff sites are more scattered, including in directions that are 90° from the paleovalley and are inconsistent with clast provenance. Our AMS results suggest west-southwest paleoflow for Peach Springs Tuff deposited within the confines of the Lost Marble paleovalley, while flow directions elsewhere are not consistent and probably affected by irregular paleotopography below the tuff. This west-southwest flow direction agrees well with the approximately west orientation of the valley margin determined from the pattern of gravel outcrops.

BGMFZ Piercing Point. The Lost Marble paleovalley serves as a valuable piercing point across the BGMFZ with which to estimate the magnitude of dextral offset. We use the mapped outcrop pattern of gravel and tuff in conjunction with AMS K3 imbrication directions to define the northern and southern margins of the Lost Marble paleovalley (fig. 10). On the west side of the fault in the Old Dad Mountains, the southern paleovalley margin is well defined by gravel outcrops and the minimum northern extent of the paleovalley can be inferred. On the east side of the fault in the Marble Mountains, the northern margin is well defined. Utilizing the northern paleovalley margin as a piercing point gives a minimum offset estimate of 24 km.

This 24-km minimum offset estimate could be augmented by ascertaining a northern paleovalley margin in the Old Dad Mountains. Unfortunately, Peach Springs Tuff and Lost Marble gravel are not preserved north of the outcrops depicted in figure 3*A*. It is also possible that the northern paleovalley margin in the Marble Mountains may project further south than our estimate (fig. 10), in better agreement with the easterly K3 direction here, again suggesting that the 24-km offset estimate is a minimum. Additionally, faults that branch from the BGMFZ east into the northern Marble Mountains in the region north of the Lost Marble paleovalley may absorb some dextral offset as part of a horsetail splay (Howard and Miller 1992), again suggesting total BGMFZ offset may exceed 24 km.

Conclusions

The Lost Marble gravel deposits of the Old Dad and Marble mountains indicate a middle Miocene paleovalley piercing point across the BGMFZ, with a minimum of 24 km of net dextral slip (fig. 10). Whereas previous indicators of cumulative dextral shear along the BGMFZ are equivocal, the newly recognized Lost Marble paleovalley is proximal to the BGMFZ and provides a more robust estimate of total BGMFZ offset than previous geologically based estimates. Furthermore, the 24-km minimum offset estimate agrees well with kinematic predictions for BGMFZ dextral slip of 21.5 km (Dokka and Travis 1990*a*) and 27 km (McQuarrie and Wernicke 2005). When considering the entire Mojave Desert portion of the ECSZ, our new 24-km offset estimate for the BGMFZ raises the geological estimate of net slip to ~67 km, consistent with the 65-km model estimate of Dokka and Travis (1990*a*), though more faults or more displacement on known faults is necessary to validate the 100-km model estimate of McQuarrie and Wernicke (2005). Further exploration of the poorly constrained late Miocene history of the eastern edge of the Mojave block may help resolve this remaining slip discrepancy.

Though the magnitude of BGMFZ offset is constrained by the Lost Marble paleovalley, initiation of BGMFZ movement is poorly dated by local features. Dextral shear measured by displacement of the Lost Marble gravel must postdate deposition of the Peach Springs Tuff (18.5 Ma), which caps the gravel. However, regional kinematic compatibility suggests that BGMFZ dextral shear may be restricted to the last 11 Ma. The 45° clockwise rotation of the eastern Transverse Ranges (Carter et al. 1987; Richard 1993) must be accommodated by distributed dextral shear across the Mojave portion of the ECSZ to the north. Also, large magnitudes of oblique extension north of the Garlock fault in the northern and central Basin and Range between 11 and 3 Ma (Snow and Lux 1999; Snow and Wernicke 2000; Niemi et al. 2001) require similar magnitude and age of dextral shear along fault blocks of the ECSZ in the Mojave (McQuarrie and Wernicke 2005). Thus, kinematic compatibility constraints suggest that dextral shear in the ECSZ, for which the BGMFZ is the eastern boundary fault, commenced at 10-11 Ma (McQuarrie and Wernicke 2005). Though largely inactive in the late Quaternary (Bedford et al. 2006), the BGMFZ must have at one time been a significant member of the ECSZ, with a time-averaged slip rate in excess of 2 mm/yr.

ACKNOWLEDGMENTS

The assistance of J. Flemming, E. Shelef, and T. Ben David made fieldwork enjoyable and productive. This work would not have been possible without

generous undergraduate senior thesis funding from the Princeton University Department of Geosciences and later support from a National Science Foundation Graduate Research Fellowship to R. O. Lease. Conversations with sundry others at the Geological Society of America Penrose Conference (Kinematics and Geodynamics of Intraplate Dextral Shear in Eastern California and Western Nevada; April 21–26, 2005, Mammoth Lakes, CA) provided a broader context for this work. Comments by J. Faulds and several anonymous reviewers refined our approach. Thanks also to the University of California, Riverside, Sweeney Granite Mountains Desert Research Center.

REFERENCES CITED

Atwater, T. 1970. Implications of plate tectonics for the Cenozoic tectonic evolution of western North America. Geol. Soc. Am. Bull. 81:3513–3536.

Atwater, T., and Stock, J. 1998. Pacific–North America plate tectonics of the Neogene southwestern United States; an update. *In* Ernst, W. G., and Nelson, C. A., eds. Integrated Earth and environmental evolution of the southwestern United States (the Clarence A. Hall Jr. volume). Columbia, MD, Bellwether, p. 393–420.

Bartley, J. M. 1990. North-south contraction of the Mojave block and strike-slip tectonics in southern California. Science 248:1398–1401.

Bedford, D. R.; Miller, D. M.; Phelps, G. A. 2006. Preliminary surficial geologic map database of the Amboy 30 × 60 minute quadrangle, California U.S. Geol. Surv. Open-File Report 2006-1165, http://pubs.usgs.gov/of/2006/1165/.

Brady, R. H. 1992. The Eastern California shear zone in the northern Bristol Mountains, southeastern California. *In* Deformation associated with the Neogene Eastern California Shear Zone, southwestern Arizona and southeastern California. Redlands, CA, San Bernardino County Museum, p. 6–10.

———. 1993. Cenozoic stratigraphy and structure of the northern Bristol Mountains, Calif. U.S. Geol. Surv. Bull. B2053, p. 25–28.

Buesch, D. C. 1989. Geochemical variations in ignimbrite phenocrysts: implications for eruption history and vent location. EOS: Trans. Am. Geophys. Union 70:1413.

———. 1991. Changes in depositional environments resulting from emplacement of a large-volume ignimbrite. Soc. Sediment. Geol. Spec. Publ. 45:139–153.

———. 1993. Feldspar geochemistry of four Miocene ignimbrites in southeastern Calif. and western Ariz. U.S. Geol. Surv. Bull. B2053, p. 55–69.

Cagnoli, B., and Tarling, D. H. 1997. The reliability of anisotropy of magnetic susceptibility (AMS) data as flow direction indicators in friable base surge and ignimbrite deposits: Italian examples. J. Volcanol. Geotherm. Res. 75:309–320.

Carter, J. N.; Luyendyk, B. P.; and Terres, R. R. 1987. Neogene clockwise tectonic rotation of the eastern Transverse Ranges, California, suggested by paleomagnetic vectors. Geol. Soc. Am. Bull. 98:199–206.

Dibblee, T. W. 1961. Evidence of strike-slip movement on northwest-trending faults in Mojave Desert, California. U.S. Geol. Surv. Prof. Paper 424-B, p. 197–198.

Davis, G. A., and Burchfiel, B. C.1973. Garlock Fault: an intracontinental transform structure, southern California. Geol. Soc. Am. Bull. 84:1407–1422

Dickinson, W. R., and Wernicke, B. P. 1997. Reconciliation of San Andreas slip discrepancy by a combination of interior Basin-Range extension and transrotation near the coast. Geology 25:663–665.

Dokka, R. K. 1983. Displacements on Late Cenozoic strike-slip faults of the central Mojave Desert, California. Geology 11:305–308.

Dokka, R. K., and Travis, C. J. 1990*a*. Late Cenozoic strike-slip faulting in the Mojave Desert, California. Tectonics 9:311–340.

———. 1990*b*. Role of the Eastern California Shear Zone in accommodating Pacific–North American plate motion. Geophys. Res. Lett. 17:1323–1326.

Ellwood, B. B. 1982.Estimates of flow direction for calc-alkaline welded tuffs and paleomagnetic data reliability from anisotropy of magnetic-susceptibility measurements—central San Juan Mountains, southwest Colorado. Earth Planet. Sci. Lett. 59:303–314.

Gamble, J. 1959*a*. Geology and mineral resources of township 8 north, ranges 11 and 12 east, San Bernardino base and meridian, San Bernardino County, California. Unpublished report and 1 : 24,000 scale map. San Francisco, Southern Pacific, 22 p.

———. 1959*b*. Geology and mineral resources of township 9 north, ranges 11 and 12 east, San Bernardino base and meridian, San Bernardino County, California. Unpublished report and 1 : 24,000 scale map. San Francisco, Southern Pacific, 18 p.

Garfunkel, Z. 1974. Model for the late Cenozoic tectonic history of the Mojave Desert, California, and for its relation to adjacent regions. Geol. Soc. Am. Bull. 85: 1931–1944.

Glazner, A. F., and Bartley, J. M. 1990. Early Miocene dome emplacement, diking, and limited tectonism in the northern Marble Mountains, eastern Mojave Desert, California. *In* Foster, J. H., and Lewis, L. L., eds. Lower Colorado River extensional terrane and Whipple Mountains. Santa Ana, CA, South Coast Geological Society, p. 89–97.

Glazner, A. F.; Nielson, J. E.; Howard, K. A.; and Miller, D. M. 1986. Correlation of the Peach Springs Tuff, a large-

volume Miocene ignimbrite sheet in California and Arizona. Geology 14:840–843.

Glazner, A. F.; Walker, J. D.; Bartley, J. M.; and Fletcher, J. M. 2002. Cenozoic evolution of the Mojave Block of Southern California. *In* Glazner, A. F.; Walker, J. D.; and Bartley, J. M., eds. Geological evolution of the Mojave Desert and southwestern Basin and Range. Geol. Soc. Am. Mem. 195:19–41.

Hendricks, J. D. 2003. Geophysics–Granite Mountains. *In* Theodore, T. G., ed. Geology and mineral resources of the east Mojave national scenic area. U.S. Geol. Surv. Bull. 2160, 84 p.

Hillhouse, J. W., and Wells, R. E. 1991. Magnetic fabric, flow directions, and source area of the lower Miocene Peach Spring tuff in Arizona, California, and Nevada. J. Geophys. Res. 96:12443–12460.

Hinz, N. H.; Faulds, J. E.; and Henry, C. D. 2009. Tertiary volcanic stratigraphy and paleotopography of the Diamond and Fort Sage mountains: constraining slip along the Honey Lake fault zone in the northern Walker Lane, northeastern California and western Nevada. *In* Oldow, J. S., and Cashman, P., eds. Late Cenozoic structure and evolution of the Great Basin–Sierra Nevada transition Geol. Soc. Am. Spec. Pap., 447 p.

Howard, K. A.; Kilburn, J. E.; Simpson, R. W.; Fitzgibbon, T. T.; Detra, D. E.; and Raines, G. L. 1987. Mineral resources of the Bristol/Granite mountains wilderness study area, San Bernadino County, Calif. U.S. Geol. Surv. Bull. 1712-C, 18 p.

Howard, K. A., and Miller, D. M. 1992. Late Cenozoic faulting at the boundary between the Mojave and Sonoran blocks: Bristol Lake area, California. *In* Deformation associated with the Neogene Eastern California Shear Zone, southwestern Arizona and southeastern California. Redlands, CA, San Bernardino County Museum Special Publication, p. 37–47.

Hrouda, F. 1982. Magnetic anisotropy of rocks and its application in geology and geophysics. Geophys. Surv. 5:37–82.

Lee, J.; Stockli, D.; Schroeder, J.; Tincher, C.; Bradley, D.; and Owen, L. 2005. Fault slip transfer in the Eastern California Shear Zone/Walker Lane Belt. *In* Geological Society of America Penrose Conference, Kinematics and geodynamics of intraplate dextral shear in eastern California and western Nevada., Mammoth Lakes, CA, April 21–26, 2005. Field guide, p. 22–72.

Le Pennec, J. L.; Chen, Y.; Diot, H.; Froger, J. L.; and Gourgaud, A. 1998. Interpretation of anisotropy of magnetic susceptibility fabric of ignimbrites in terms of kinematic and sedimentological mechanisms; an Anatolian case study. Earth Planet. Sci. Lett. 157: 105–127.

MacDonald, W. D., and Palmer, H. C. 1990. Flow directions in ashflow tuffs: a comparison of geological and magnetic susceptibility measurements, Tshirege member (upper Bandelier tuff), Valles caldera, New Mexico, USA. Bull. Volcanol. 53:45–59.

Mark, D. M. 1973. Analysis of axial orientation data, including till fabrics. Geol. Soc. Am. Bull. 84: 1369–1373.

McClusky, S. S.; Bjornstad, S.; Hager, B.; King, R.; Meade, B.; Miller, M.; Monastero, F.; and Souter, B. 2001. Present day kinematics of the Eastern California Shear Zone from a geodetically constrained block model. Geophys. Res. Lett. 28:3369–3372.

McQuarrie, N. 2002. Initial plate geometry, shortening variations, and evolution of the Bolivian orocline. Geology 30:867–870.

McQuarrie, N.; Stock, J. M.; Verdel, C.; and Wernicke, B. P. 2003. Cenozoic evolution of Neotethys and implications for the causes of plate motions. Geophys. Res. Lett. 30:2036.

McQuarrie, N., and Wernicke, B. P. 2005. An animated tectonic reconstruction of southwestern North America since 36 Ma. Geosphere 1:147–172.

Miall, A. D. 1996. The geology of fluvial deposits: sedimentary facies, basin analysis, and petroleum geology. Berlin, Springer, 582 p.

Miller, D. M. 1993. Cenozoic deposits in the Lava Hills and southern Bristol Mountains, southeastern Calif. U.S. Geol. Surv. Bull. B2053, p. 99–107.

Miller, D. M.; Miller, R. J.; Nielsen, J. E.; Wilshire, H. G.; Howard, K. A.; and Stone, P. 2003. Geological map of the east Mojave national scenic area, California. *In* Theodore, T. G., ed. Geology and mineral resources of the east Mojave national scenic area, San Bernardino County, Calif. U.S. Geol. Surv. Bull. 2160, plate 1.

Molnar, P., and Tapponnier, P. 1975. Cenozoic tectonics of Asia; effects of a continental collision. Science 189: 419–426.

Nemec, W., and Steele, R. J. 1984. Alluvial and coastal conglomerates: their significant features and some comments on gravelly mass-flow deposits. *In* Koster, E. H., and Steel, R. J., eds. Sedimentology of gravels and conglomerates. Can. Soc. Pet. Geol. Mem. 10:1–31.

Nielson, J. E.; Lux, D. R.; Dalrymple, G. B.; and Glazner, A. F. 1989. Age of the Peach Springs Tuff, southeastern California and western Arizona. J. Geophys. Res. 95: 571–580.

Niemi, N. A.; Wernicke, B. P.; Brady, R. J.; Saleeby, J. B.; and Dunne, G. C. 2001. Distribution and provenance of the middle Miocene Eagle Mountain Formation, and implications for regional kinematic analysis of the Basin and Range province. Geol. Soc. Am. Bull. 113: 419–442.

Oldow, J. S. 1992. Late Cenozoic displacement partitioning in the northwest Great Basin. *In* Craig, S. D., ed. Proceedings, Walker Lane Symposium, Structure, tectonics, and mineralization of the Walker Lane. Geological Society of Nevada, p. 17–52.

Oldow, J. S.; Aiken, C. L. V.; Hare, J. L.; and Hardyman, R. F. 2001. Active displacement transfer and differential block motion within the central Walker Lane, western Great Basin. Geology 29:19–22.

Oskin, M., and Iriondo, A. 2004. Large magnitude transient strain accumulation on the Blackwater Fault, Eastern California Shear Zone. Geology 32:313–316.

Oskin, M., and Stock, J. 2003. Pacific–North America

plate motion and opening of the Upper Delfín basin, northern Gulf of California, Mexico. Geol. Soc. Am. Bull. 115:1173–1190.

Palmer, H. C.; MacDonald, W. D.; Gromme, C. S.; and Ellwood, B. B. 1996. Magnetic properties and emplacement of the Bishop Tuff, California. Bull. Volcanol. 58: 101–116.

Palmer, H. C.; MacDonald, W. D.; and Hayatsu, A. 1991. Magnetic, structural and geochronological evidence bearing on volcanic sources and Oligocene deformation of ash flow tuffs, northeast Nevada. J. Geophys. Res. 96:2185–2202.

Pardo-Casas, F., and Molnar, P. 1987. Relative motion of the Nazca (Farallon) and South American plates since Late Cretaceous time. Tectonics 6:233–248.

Rees, A. I. 1968. Production of preferred orientation in a concentrated dispersion of elongated and flattened grains. J. Geol. 76:457–465.

Richard, S. M. 1993. Palinspastic reconstruction of southeastern California and southwestern Arizona for the Middle Miocene. Tectonics 12:830–854.

Sauber, J.; Thatcher, W.; Solomon, S.; and Lisowski, M. 1994. Geodetic slip rate for the Eastern California Shear Zone and the recurrence time of Mojave desert earthquakes. Nature 367:264–266.

Savage, J. C.; Lisowski, M.; and Prescott, W. 1990. An apparent shear zone trending north-northwest across the Mojave desert in to Owens Valley, eastern California. Geophys. Res. Lett. 17:2113–2116.

Şengör, A. M. C. 1990. Plate tectonics and orogenic research after 25 years: a Tethyan perspective. Earth Sci. Rev. 27:1–201.

Şengör, A. M. C., and Natal'in, B. A. 1996. Paleotectonics of Asia: fragments of a synthesis, *In* Yin, A., and Harrison, T. M., eds. The tectonic evolution of Asia. New York, Cambridge University Press, p. 486–640.

Snow, J. K., and Lux, D. R. 1999. Tectono-sequence stratigraphy of Tertiary rocks in the Cottonwood Mountains and northern Death Valley area, California and Nevada. *In* Wright, L. A., and Troxel, B. W., eds. Cenozoic basins of the Death Valley region. Geol. Soc. Am. Spec. Pap. 333:17–64.

Snow, J. K., and Wernicke, B. P. 2000. Cenozoic tectonism in the central Basin and Range: magnitude, rate and distribution of upper crustal strain. Am. J. Sci. 300: 659–719.

Stewart, J. H. 1988, Tectonics of the Walker Lane belt western Great Basin—Mesozoic and Cenozoic deformation in a zone of shear. *In* Ernst, W. G., ed. Metamorphism and crustal evolution of the Western United States. Englewood Cliffs, NJ, Prentice Hall, p. 683–713.

Tapponnier, P.; Peltzer, G.; Le Dain, A. Y.; and Armijo, R. 1982. Propagating extrusion tectonics in Asia: New insights from simple experiments with plasticine. Geology 10:611–616.

Valentine, G. A.; Buesch, D. C.; and Fisher, R. V. 1989. Basal layered deposits of the Peach Springs Tuff, northwestern Arizona, USA. Bull. Volcanol. 52: 565–569.

Walker, J. D.; Bartley, J. M.; and Glazner, A. F. 1990. Large-magnitude Miocene extension in the central Mojave Desert: implications for Paleozoic to Tertiary paleogeography and tectonics. J. Geophys. Res. 95:557–569.

Wells, R. E., and Hillhouse, J. W. 1989. Paleomagnetism and tectonic rotation of the Lower Miocene Peach Springs Tuff: Colorado Plateau, Arizona, to Barstow, California. Geol. Soc. Am. Bull. 101:846–863.

Wernicke, B. P., and Snow, J. K. 1998. Cenozoic tectonism in the central Basin and Range: motion of the Sierran–Great Valley Block. Int. Geol. Rev. 40:403–410.

Wooden, J. L., and Miller, D. M. 1990. Chronologic and isotopic framework for Early Proterozooic crustal evolution in the eastern Mojave Desert region, SE California. J. Geophys. Res. 95:20133–20146.

Young, R. A., and Brennan, W. J. 1974. The Peach Springs Tuff: its bearing on the structural evolution of the Colorado Plateau and development of Cenozoic drainage in Mohave County, Arizona. Geol. Soc. Am. Bull. 85:83–90.